Supplementary Information

Eolian dust input to the Subarctic North Pacific

Sascha Serno, Gisela Winckler, Robert F. Anderson, Christopher T. Hayes, David McGee, Björn Machalett, Haojia Ren, Susanne M. Straub, Rainer Gersonde, Gerald H. Haug

1. Lithogenic contributions to Bering Sea sediments

Fine-grained lithogenic material in the Bering Sea is mainly derived from riverine input from rivers in Alaska and northeast Siberia and the surrounding volcanic arcs, rather than East Asian eolian dust (e.g., Asahara et al., 2012; Fullam et al., 1973; VanLaningham et al., 2009). Concentrations of ^{4}He are around an order of magnitude higher in the northern Bering Sea stations 13 and 15-19 compared to the stations from the northwest and northeast Subarctic North Pacific (SNP; Supplementary Dataset 1), which cannot be the result of East Asian dust input, but is more likely of riverine input of continental crust-like sediments. Since we cannot derive an estimate of the importance of this riverine contribution for the single stations in the Bering Sea, we excluded all Bering Sea stations (stations 10-22) from the calculation of dust contributions.

2. Geochemical methodology and background

2.1 Grain size distributions

Prior to grain size analyses, biogenic components were removed by a leaching procedure described in McGee et al. (2013), including leaching of organic matter

with concentrated H_2O_2, followed by $CaCO_3$ leaching with 1M HCl and removal of biogenic opal with 2M Na_2CO_3 for 5 hours in a hot bath with a constant temperature of 85 ˚C, followed by multiple centrifuging and decanting steps. Particle size distributions were measured using a Beckman-Coulter LS 13 320 laser diffraction particle size analyzer at the Bentley University Particle Size Laboratory following the method described by Machalett et al. (2008). An auto-prep station was used to measure each sample (2-3 aliquots per sample, 5 measurements per aliquot) under equal conditions using the standard operating method Bentley-BM-v13 (Machalett, 2010). Grain size data are reported in 92 bins ranging from 0.38 to 2000 µm. Coefficients of variation were <0.5% for the 5 measurements per aliquot and 2-5% for the 2-3 aliquots for all samples.

2.2 Grain size endmember modeling

Grain size data were used to provide upper limits on the fraction of eolian dust in each sample. Grain size distributions for the samples were modeled as the sum of three endmember Weibull distributions following the approach of McGee et al. (2013). Briefly, three Weibull distributions that together provided the best fit to the data were determined using an iterative least-squares technique. This grain size modeling approach has been found to closely approximate the measured size distribution of dust and loess (Sun et al., 2004; Zobeck et al., 1999). The resulting endmembers EM1-EM3 have modal values of 4, 25, and 44 µm, respectively. The weighting of these endmembers that provided the best fit to each individual sample was then determined; these weighting factors express our best estimate of the proportion of each sample that reflects contributions from a given endmember. The mean residual between our modeled distributions and the actual distributions is 0.16%, or approximately 10% of the average value of each grain size bin. The distributions of the best-fit endmembers and of the mean residual of our fits to the samples are shown in Supplementary Fig. S1.

2.3 Helium isotopes

Terrestrial ^4He ($^4He_{terr}$) has been successfully used to reconstruct eolian dust in marine sediments (e.g., Marcantonio et al., 2009; McGee, 2009; Mukhopadhyay et al., 2001; Patterson et al., 1999; Winckler et al., 2005, 2008), Antarctic ice (Winckler and Fischer, 2006), and corals (Bhattacharya, 2012; Mukhopadhyay and Kreycik, 2008). $^4He_{terr}$ is continuously produced by α-decay of U/Th series elements within the continental rock matrix and is concentrated in accessory minerals like zircon or apatite (Andrews, 1985; Mamyrin and Tolstikhin, 1984; Patterson et al., 1999; Winckler et al., 2008). $^4He_{terr}$ concentrations in East Asian dust originating from continental rocks range between ~1000-10000 ncc STP g^{-1} (McGee, 2009; ncc STP g^{-1} = nano cubic centimeter per gram at standard temperature and pressure) and are two to three orders of magnitude higher than concentrations in volcanic rocks, for example from Kamchatka (~5-10 ncc STP g^{-1}; Kurz et al., 2004; Mamyrin and Tolstikhin, 1984; Patterson et al., 1999); since ^4He is not adsorbed onto mineral surfaces, nor scavenged by particles or incorporated into biogenic phases, its sedimentary concentration is directly proportional to continental material (Farley, 1995; Marcantonio et al., 1995, 1998; Mukhopadhyay and Kreycik, 2008; Patterson et al., 1999) and insensitive to contributions of volcanic materials.

Helium isotopes in marine sediments are a binary mixture of continental material and extraterrestrial interplanetary dust particles (IDPs). $^4He_{terr}$ concentrations of each sample i can be calculated using a two-component mixing model with the measured ^4He concentrations ($^4He_{meas}$) and helium isotope ratio [$(^3He/^4He)_{meas}$] (Patterson et al., 1999; Winckler et al., 2005):

$$^4He_{terr}\,(i) = {}^4He_{meas}\,(i) \times \frac{(^3He/^4He)_{meas}\,(i) - (^3He/^4He)_{IDP}}{(^3He/^4He)_{terr} - (^3He/^4He)_{IDP}} \qquad \text{(S1)}$$

with $(^3He/^4He)_{IDP}$ = ratio of IDPs = 2.4 x 10^{-4} (Nier and Schlutter, 1990, 1992), and $(^3He/^4He)_{terr}$ = ratio of continental crust material = 3 x 10^{-8} (Farley, 2001; Mamyrin and Tolstikhin, 1984).

Between 40 and 700 mg of freeze-dried and hand-crushed bulk sediment was wrapped in aluminum foil cups, loaded into the vacuum furnace of the gas inlet system, and analyzed on a MAP 215-50 mass spectrometer at Lamont-Doherty Earth Observatory (LDEO) following procedures described in Winckler et al. (2005). Calibration was performed every 4-5 samples using a known volume of a standard with an isotopic ratio of 16.45 R_A (R_A = atmospheric isotopic ratio = 1.384 x 10^{-6}). Standard reproducibility for the $^4He_{meas}$ and $(^3He/^4He)_{meas}$ was ~0.5% and 1.5% (1σ), respectively. Procedural blanks yielded 0.1-0.2 ncc STP of ^4He with atmospheric isotopic composition and represented blank corrections of <1% ^4He for most of the samples, with occasional corrections up to 7%.

For all but 5 samples we analyzed 3-5 replicates. Mean values for ^4He and $^3He/^4He$ were calculated after removing outliers using Chauvenet's criterion (Taylor, 1997). Standard deviations for mean $^4He_{meas}$ concentrations varied between 0.39 and 64.26%, averaging 8.74%. Reproducibility for $(^3He/^4He)_{meas}$ varied between 0.94 and 105.47%, averaging 33.27% (1σ). This reproducibility is similar to uncertainties found in other studies (Farley et al., 1997; Torfstein, 2012) and reflects the fact that extraterrestral ^3He, the dominant source of ^3He, is hosted by a relatively small number of individual IDPs that are not representatively sampled. The contribution of $^4He_{terr}$ to $^4He_{meas}$ is >95.5% for all samples. The high $^4He_{terr}$ contribution results in insensitivity of calculated $^4He_{terr}$ concentrations to different values of $(^3He/^4He)_{terr}$ that could be chosen from the range of possible endmember values. Concentrations of $^4He_{terr}$ vary by <0.2% when using the mean helium isotope ratio of the East Asian dust source fine size fractions (~3 x 10^{-7}; McGee, 2009). The order of magnitude difference between the East Asian dust helium isotope ratio and $(^3He/^4He)_{terr}$ of the bulk continental crust (3 x 10^{-8}; e.g., Farley, 2001; Mamyrin and Tolstikhin, 1984) is the result of

the grain size effect of $^{4}He_{terr}$, with increasing concentrations with increasing grain size, but fairly constant ^{3}He (McGee, 2009).

2.4 Uranium/Thorium isotopes

Excess ^{230}Th ($xs^{230}Th_0$) has been established as a constant-flux proxy (e.g., Anderson et al., 2006; Bacon, 1984; Francois et al., 2004; Henderson et al., 1999; McGee et al., 2007). The ^{230}Th profiling method is described in detail in Francois et al. (2004). Briefly, ^{230}Th is produced in the water column by α-decay of ^{234}U and shows low concentrations in seawater as a result of efficient particle scavenging (e.g., Anderson et al., 1983; Bacon and Anderson, 1982; Francois et al., 2004; Henderson et al., 1999). Therefore, its scavenged flux to the seafloor can be assumed to be approximately equal to its production rate in the overlying water column (β_{230} = 2.67 x 10^{-5} dpm cm^{-3} kyr^{-1}; Francois et al., 2004). Mass accumulation rates (MARs) for a constituent i, MAR_i, with a concentration c_i in the sediment deposited at a specific water depth z can be calculated by:

$$MAR_i = \frac{c_i \times \beta_{230} \times z}{xs^{230}Th_0} \qquad \text{(S2)}$$

$xs^{230}Th_0$ is the excess sedimentary ^{230}Th concentration in dpm/g corrected for continuing decay, the fraction supported by uranium within lithogenic material (mean detrital $^{238}U/^{232}Th$ = 0.5 ± 0.1; Taguchi and Narita, 1995), and the fraction of the in-situ produced ^{230}Th by decay of authigenic ^{238}U (Anderson et al., 2006; Francois et al., 2004). Corrections for the detrital fraction of ^{230}Th are ~10%. We assumed an age of 0 years for the sediments, resulting in no correction for ^{230}Th decay or in-situ ^{230}Th production due to authigenic U decay.

The constant-flux proxy offers advantages over the conventional stratigraphic MAR estimates in that the ^{230}Th-normalized fluxes are insensitive to lateral sediment redistribution and less sensitive to age model uncertainties than

stratigraphic MAR estimates, and do not rely on the determination of dry bulk density (Anderson et al., 2006; Francois et al., 2004; Henderson et al., 1999).

In the last ~10 years, ^{232}Th has been successfully used as a dust proxy in marine sediments (e.g., Anderson et al., 2006; Kohfeld and Chase, 2011; Marcantonio et al., 2001; McGee, 2009; McGee et al., 2007, 2013; Winckler et al., 2008; Woodard et al., 2012) and seawater (Hayes et al., 2013; Hsieh et al., 2011). ^{232}Th in sediments and seawater is purely of detrital origin and has no association with biogenic material (e.g., Brewer et al., 1980; Woodard et al., 2012). Accessory and clay minerals have been proposed as its main host phases (Herron and Matteson, 1993; McGee, 2009). Concentrations of ^{232}Th in volcanic material are almost an order of magnitude lower than in eolian dust (Gale et al., 2013; Taylor and McLennan, 1985).

Approximately 100 mg of freeze-dried and hand-crushed bulk sediment from all 37 INOPEX samples was weighed into 50 ml Teflon beakers and spiked with ^{229}Th and ^{236}U prior to a complete acid digestion and anion exchange chromatography following the method of Fleisher and Anderson (2003). Samples were analyzed for U/Th isotopes by isotope dilution on a high-resolution VG Elemental Axiom ICP-MS at LDEO. ^{238}U concentrations were calculated using the measured ^{235}U/^{236}U ratio and a ^{238}U/^{235}U ratio of 137.88 for the SRM129 standard (Steiger and Jäger, 1977), measured with every batch of 18 samples and one procedural blank. Blank corrections were <1.61% for ^{230}Th, <0.56% for ^{232}Th and <0.63% for ^{238}U. Mean replicate reproducibility was 3.19% (1σ) for ^{230}Th, 3.27% (1σ) for ^{232}Th, and 1.97% (1σ) for ^{238}U.

2.5 Rare earth elements

Lithogenic sediment provenance is the main controlling factor for rare earth element (REE) variability in marine sediments (e.g., Chen et al., 2003; Taylor and

McLennan, 1985). REEs have been successfully used in provenance studies of East Asian dust material (Bailey, 1993; Ferrat et al., 2011; Gallet et al., 1996, 1998; Maeda et al., 2007; Nakai et al., 1993; Olivarez et al., 1991; Otosaka et al., 2004; Shigemitsu et al., 2007; Weber et al., 1996). REEs are mainly concentrated in accessory minerals like zircon, although some clay minerals are also REE enriched (e.g., Ferrat et al., 2011; Gallet et al., 1996; Moreno et al., 2006).

Around 100 mg of finely ground bulk sediment from the INOPEX station and dust source samples was weighed into 15 ml screw-top Savillex® Teflon vials. The rock powder was initially wetted with 15.9M HNO_3 and evaporated to a small fluid volume on a hotplate at ~150 °C. Then 5 ml 28.9M HF were added, the vials were tightly sealed and put back on the hotplate for 3.5 hours at ~200-250 °C. After 2 hours, the vials were removed from the hotplate and shaken occasionally. To drive off HF and further decompose the sediment, 2 ml 11.7M $HClO_4$ were added to the vials and they were put back on the hotplate uncapped. Following typical perchloric acid fume formation, a mixture of 1 ml 28.9M HF, 1 ml 15.9M HNO_3 and 1 ml 11.7M $HClO_4$ was added to the vials and the acid mixture was heated to perchloric acid fume formation before evaporating the samples with 0.46M HNO_3 four times at ~150 °C to dissolve remaining fluorides. The residue was re-dissolved using 0.46M HNO_3, transferred into 15 ml tubes and diluted to 10 ml with 0.46M HNO_3. From this initial solution, a solution diluted by a factor of 1000 was created for the measurements of the REEs, analyzed on a VG PQ ExCell Quadropole ICP-MS at LDEO. Indium was added as an internal standard for drift corrections. Standard additions were used for standardization. BaO interferences on Eu were suitably corrected by using the isotopic abundance of Ba. Three procedural blanks were measured with each batch, with blank corrections of <2.5% for all REEs except Eu (<7.6%). Mean replicate reproducibility is <4 % (1σ) for La, Ce, Eu, Tb, Ho, Er, Tm, Yb and Lu and <6% (1σ) for Pr, Nd, Sm, Gd and Dy.

In addition to replicate measurements of the INOPEX samples, we processed and ran two certified reference rock samples, W-2 (U.S. Geological Survey) and JA-2 (Geological Survey of Japan), and compared results with means of reported values from the GeoReM database for geological and environmental reference materials (http://georem.mpch-mainz.gwdg.de/). For W-2, all REEs fall within 3% of the reported values except for Pr, Tb, Dy and Yb (within 4.8%). For JA-2, concentrations of Pr, Nd, Sm, Eu, Tb, Tm and Lu are within 3% and of La, Ce, Gd, Dy, Ho, Er and Yb within 6.1% of the reported means (Supplementary Table S2).

For station samples 31, 37 and 40 characterized by high calcium carbonate contents, we performed a leaching procedure slightly modified from the one described by Gutjahr et al. (2007) to remove foraminifera and Fe-Mn oxyhydroxide coatings prior to the acid digestion. It has been shown that REE concentrations in the non-detrital phase of calcareous sediments, primarily REE included in the foraminiferal calcite matrix and associated with authigenic Fe-Mn-rich phases adsorbed onto the surface of foraminifera tests, can obscure the lithogenic REE signal in marine sediments (e.g., Gutjahr et al., 2007; Palmer, 1985; Roberts et al., 2012). Calcium carbonate was removed by leaching ~250 mg of finely ground sediment in 50 ml centrifuge tubes three times with 15 ml of a 52:48 mixture of 1M sodium acetate buffer and 1M acetic acid on a shaker table at room temperature for 5 hours, followed by three repeats of centrifuging and rinsing the samples with milli-Q water. Fe-Mn oxyhydroxide coatings were dissolved by leaching the samples two times on a shaker table at room temperature for 3 hours in 15 ml of a 0.05M hydroxylamine hydrochloride – 15% distilled acetic acid – 0.03M sodium-ethylenediaminetetraacetic acid solution buffered to pH 4 with analytical grade sodium hydroxide. The samples were then centrifuged and rinsed with milli-Q four times before being transferred to 15 ml screw-top standard Savillex® Teflon vials for the acid digestion.

2.6 Calcium carbonate and biogenic opal

Calcium carbonate concentrations were measured using a CM5012 CO_2 Coulometer at LDEO. A pure carbonate standard showed long-term reproducibility of 0.31% (1σ) of the mean value. Biogenic opal was measured by alkaline extraction and molybdate-blue spectrophotometry at LDEO following the procedure described in Mortlock and Froelich (1989). Long-term reproducibility of a biogenic opal standard from the Oregon State University was 3.4% (1σ) of the mean value.

2.7 Salt correction

We corrected the measured helium isotope, U/Th isotope, REE, calcium carbonate and biogenic opal data in the INOPEX samples for salt content. Bottom-water salinity was measured at the INOPEX stations. Salt corrections for a constituent [X] in sample i were performed using:

$$\text{Salt content}_i\ (\text{g}) = \frac{\text{Water loss through freeze drying}_i\ (\text{g})}{\left(1 - \frac{\text{bottom-water salinity}_i}{1000}\right)} \times \frac{\text{bottom-water salinity}_i}{1000} \quad \text{(S3)}$$

$$[X]_{\text{salt-corrected,i}} = \frac{[X]_{\text{measured, i}}}{\left(1 - \frac{\text{Salt content}_i}{\text{Dry weight}_i}\right)} \quad \text{(S4)}$$

All salt values and uncorrected and salt-corrected concentrations are available in Supplementary Dataset 1.

3. Dust sources for long-range atmospheric transport to the Subarctic North Pacific

Arid regions in China and Mongolia are considered to be the dominant sources of eolian dust input to the SNP (Duce et al., 1980; Husar et al., 2001; Sun et al., 2001; Tanaka and Chiba, 2006; Uno et al., 2011). These regions are characterized by a number of dry lakebeds and alluvial deposits (Pye and Zhou, 1989). The Taklimakan desert in northwest China is suggested to be one of the most important sources for long-range eolian dust transport in the Northern Hemisphere (Bory et al., 2002, 2003; Nagashima et al., 2007, 2011; Nakano et al., 2004; Prospero et al., 2002; Pye and Zhou, 1989; Sun et al., 2001; Uno et al., 2011; Yumimoto et al., 2009; Zhang et al., 1998; Zhao et al., 2006). Dust from this source area is uplifted into the middle and upper troposphere and transported to the North Pacific Ocean by the strong westerly jet stream (Nakano et al., 2004; Sun et al., 2001). Eolian dust from the Gobi and adjacent deserts in southern Mongolia and northern China, including the Badain Jaran and Tengger deserts, are primarily transported southeast- and eastward below 3000 m in the atmosphere (Bory et al., 2002; Sun et al., 2001; Yumimoto et al., 2009). These desert areas are the primary dust sources for the Chinese Loess Plateau (Sun et al., 2008). Dust from these sources can also be entrained into the middle troposphere and transported far distances, as has been shown in studies from East Asia and the North Pacific Ocean (Eguchi et al., 2009; Husar et al., 2001; Nagashima et al., 2007, 2011; Uno et al., 2011; Wang et al., 2004; Zhang et al., 1998; Zhao et al., 2006), North America (Husar et al., 2001; McKendry et al., 2001; Uno et al., 2011; Zdanowicz et al., 2006), and Greenland (Biscaye et al., 1997; Bory et al., 2002, 2003).

The Mongolian Gobi and large Chinese loess regions have generally been ruled out as potential sources for long-range eolian dust transport (Bory et al., 2003; Laurent et al., 2005; Svensson et al., 2000). A contribution of Mongolian Gobi (MG) dust to stations in the northern or western part of the INOPEX cruise track cannot be conclusively excluded from the surface sediment data available;

however, if the MG samples are representative for this source, the INOPEX sediment samples do not support its importance since a number of samples from the Southern Transect would clearly fall outside the mixing line between the volcanic endmember and a Mongolian Gobi dust endmember for all three geochemical tracers (Figs. 3, 4). Therefore, the Mongolian Gobi source samples have been generally excluded from the dust fraction determinations.

Additional minor eolian dust input from sources in North Africa, Middle East and Central Asia to the SNP has been suggested (e.g., Creamean et al., 2013; Hsu et al., 2012; Tanaka and Chiba, 2006). There are presently no ^{232}Th and ^{4}He data and only a very small number of REE data available for these sources. A study of REE compositions in North African dust source samples indicates a similar geochemical signature compared to the East Asian dust sources (Moreno et al., 2006). A contribution of western North American eolian dust can be excluded for the INOPEX samples (e.g., Jones et al., 1994; Rea and Hovan, 1995). Therefore, a representation of eolian dust input to the SNP by East Asian dust sources is a justified approach for the lithogenic component deconvolution in the INOPEX sediment samples.

4. Supplementary Information for the dust fraction determinations

4.1 $^{4}He_{terr}$ and ^{232}Th approaches

Concentrations of $^{4}He_{terr}$ and ^{232}Th in the 0-4 and 4-8 µm size fractions of the Taklimakan (TK-074, TK-083, TK-103, TK-116), Badain Jaran (BJ-024) and Tengger desert (TG-018) as well as Mongolian Gobi samples (MG-06, MG-17, MG-23) show high variability between 1100 and 6215 ncc STP g^{-1} and ~8-20 ppm, respectively (Fig. 3; McGee, 2009; for sample locations see Supplementary Fig. S2). Results of MG-06 are not shown in Figs. 3 and 4 because there are no ^{232}Th size fraction data available for this sample. The weighted mean of the 0-4

and 4-8 μm size fractions from Taklimakan desert samples TK-074, TK-083 and TK-103 and Inner Mongolian samples BJ-024 from the Badain Jaran and TG-018 from the Tengger desert, with all size fractions equally contributing to the mean value, falls on the regression line of the 26 selected INOPEX core-top sediment samples from the Kamchatka, Alaska and Southern Transects, excluding station 26 (Fig. 3). This indicates that these East Asian dust sources proposed as the most important sources for long-range eolian dust transport to the SNP can explain the bulk average dust deposition at all INOPEX station for the dust proxies $^{4}He_{terr}$ and ^{232}Th.

The size fraction samples show a clear grain size effect for both $^{4}He_{terr}$ and ^{232}Th. $^{4}He_{terr}$ concentrations increase with increasing grain size and ^{232}Th concentrations decrease with decreasing grain size (Fig. 3). These findings demonstrate that careful consideration of grain size is necessary in using dust endmembers to calculate dust fluxes based on $^{4}He_{terr}$ and ^{232}Th concentrations in marine sediments. Size fraction data of $^{4}He_{terr}$ from the Taklimakan desert sample TK-116 (3895 and 6215 ncc STP g^{-1} for the 0-4 and 4-8 μm size fractions, respectively; McGee, 2009) are two to three times higher compared to the other three Taklimakan desert samples TK-074, TK-083 and TK-103. The reason for the higher $^{4}He_{terr}$ concentrations is presently unknown. Because ^{232}Th concentrations in the TK-116 size fraction samples are not particularly high (16 and 13 ppm for the 0-4 and 4-8 μm size fractions, respectively; McGee, 2009), the He and Th compositions of sample TK-116 are not consistent with the endmember indicated by the INOPEX core-top sediment samples; we therefore assume that this sample is not representative of the Taklimakan dust source to the SNP and excluded it from the dust endmember calculation. This source sample is not shown in Figs. 3 and 4.

4.2 REE approach

For the REE approach, we combined the data from the 0-4 µm size fraction of TK-074, TK-083, TK-103, BJ-024 and TG-018 with 4-16 µm size fractions of TK-074, TK-103, BJ-024 and TG-018 as well as 4-8 µm size fractions of sample TK-083 (Ferrat et al., 2011; this study). Similar to $^{4}He_{terr}$ and ^{232}Th, REEs show a clear grain size effect and are depleted in fractions >32 µm compared to finer sizes (e.g., Ferrat et al., 2011; Gallet et al., 1998; Honda et al., 2004; McLennan, 1989), probably as a result of changes in the mineral composition in the different size fractions. Dominant REE hosts like accessory or clay minerals are concentrated in the fine-grained fractions (e.g., Condie, 1991; McLennan, 1989; Taylor and McLennan, 1985). REE concentrations in the <4 and 4-16 µm from the East Asian dust source samples are almost identical (Ferrat et al., 2011). We determined the mean dust endmember from the same size fractions from the same source samples used for the $^{4}He_{terr}$ and ^{232}Th approaches, with errors representing the 1σ uncertainties.

For the estimation of the volcanic endmember values from the volcanic ash layer compilations from ODP sites 881, 882 and 887, outliers from the volcanic ash layer compilations have been excluded based on specific REE pattern characteristics of the LREEs (light REEs; La, Ce, Pr, Nd), HREEs (heavy REEs; Ho, Er, Tm, Yb, Lu) and MREEs (middle REEs; Sm, Eu, Gd, Tb, Dy) observed in the INOPEX samples from the specific volcanic regions. Resulting mean REE pattern values with 1σ uncertainties for the volcanic endmembers are shown in Supplementary Fig. S3 as grey filled areas.

For volcanic region 1, ash layers with UNE numbers 4, 9, 15, 22, 27, 30, 33, 39 and 45 from ODP site 881 (47.1 °N, 161.5 °E, 5530 m water depth; Fig. 1) east of the Kurile Islands have been used to calculate the mean endmember (Cao et al., 1995a). Region 2 mean volcanic endmember values are the result of ash layers with UNE numbers 54, 55, 57, 73, 76, 78, 79 and 81 from ODP site 882 (50.4 °N, 167.6 °E, 3244 m water depth; Fig. 1) on the Detroit Seamount south of the western Aleutian Trench (Cao et al., 1995a). Volcanic ash layers

163, 168, 169, 174, 175, 178 and 179 from ODP site 887 (54.4 °N, 211.6 °E, 3631 m water depth; Fig. 1) from the Patton Seamounts in the northeast SNP contribute to the mean volcanic endmember of region 3 (Cao et al., 1995b).

Ash layers at sites 881 and 882 are mainly rhyolitic in their composition, but the majority of volcanic rocks from the Kurile Islands and Kamchatka are calcalkaline basalts and andesites typical for island arcs (e.g., Bailey et al., 1989; Bindeman et al., 2004; Cao et al., 1995a; Scheidegger et al., 1980), supporting a transport-related compositional change. For ODP site 881, the predominant source of the ash layers has been suggested to be the Kurile-Kamchatka arc region, different to site 882 where both the Kurile-Kamchatka and the relatively inactive western Aleutian arc contribute (Cao et al., 1995a). Ash layers at site 887 range in their composition from basaltic andesites to rhyolites and are predominantly of Aleutian and Alaskan origin (Cao et al., 1995b).

5. Bioturbation model - MATLAB code

Below we provide the MATLAB code for the applied simple bioturbation model with short descriptions for the model parameters:

```
dt=0.02; %time step in kyr
v=5; %sedimentation rate in cm/kyr
dx=dt*v; %distance step (determined by time step and sedimentation rate)
t_final=20; %duration of model in kyr
x_final=t_final*v; %length of model in cm
x=0:dx:x_final; %for plotting results
t=0:dt:t_final; %for plotting results
steps=t_final/dt+1;
db=5; %bioturbation depth in cm
bsteps=db/dx; %number of time steps in bioturbated interval
```

```
%set up input signal
%initially create vector of zeros
sig=zeros(steps); %signal length is same as number of time steps
sig(:)=1;
sig(1:582)=4; %creates a simple two-step function with a signal of 1 for the
                time after 11.64 kyr BP and 4 for time before 11.64 kyr BP

%set up initial sediment column
sed=zeros(length(x),length(t));
sed(1:bsteps,1)=((sum(sed(1:bsteps,1))+sig(1))/bsteps);

%now build sediment column with bioturbated input signal
for i=2:steps
    sed(1:bsteps,i)=((sum(sed(1:bsteps-1,i-1))+sig(i))/bsteps);
    for j=bsteps+1:steps
        sed(j,i)=sed(j-1,i-1);
    end
end

%plot results
plot(t,sed(:,steps));
```

References

Anderson, R.F., Bacon, M.P., Brewer, P.G., 1983. Removal of ^{230}Th and ^{231}Pa from the open ocean. Earth Planet. Sc. Lett. 62, 7-23.

Anderson, R.F., Fleisher, M.Q., Lao, Y., 2006. Glacial-interglacial variability in the delivery of dust to the central equatorial Pacific Ocean. Earth Planet. Sc. Lett. 242, 406-414.

Andrews, J.N., 1985. The isotopic composition of radiogenic helium and Its use to study groundwater movement in confined aquifers. Chem. Geol. 49, 339-351.

Asahara, Y., Takeuchi, F., Nagashima, K., Harada, N., Yamamoto, K., Oguri, K., Tadai, O., 2012. Provenance of terrigenous detritus of the surface sediments in the Bering and Chukchi Seas as derived from Sr and Nd isotopes: Implications for recent climate change in the Arctic regions. Deep-Sea Res. II 61-64, 155-171.

Bacon, M.P., 1984. Glacial to interglacial changes in carbonate and clay sedimentation in the Atlantic Ocean estimated from ^{230}Th measurements. Chem. Geol. 46, 97-111.

Bacon, M.P., Anderson, R.F., 1982. Distribution of thorium isotopes between dissolved and particulate forms in the deep sea. J. Geophys. Res.-Oc. 87, 2045-2056.

Bailey, J.C., 1993. Geochemical history of sediments in the northwestern Pacific Ocean. Geochem. J. 27, 71-90.

Bailey, J.C., Frolova, T.I., Burikova, I.A., 1989. Mineralogy, geochemistry and petrogenesis of Kurile island-arc basalts. Contrib. Mineral Petrol. 102, 265-280.

Bhattacharya, A., 2012. Application of the Helium isotopic system to accretion of terrestrial and extraterrestrial dust through the Cenozoic. Ph.D. Thesis, Harvard University, Cambridge, MA.

Bindeman, I.N., Ponomareva, V.V., Bailey, J.C., Valley, J.W., 2004. Volcanic arc of Kamchatka: a province with high-$\delta^{18}O$ magma sources and large-scale $^{18}O/^{16}O$ depletion of the upper crust. Geochim. Cosmochim. Ac. 68, 841-865.

Biscaye, P.E., Grousset, F.E., Revel, M., Van der Gaast, S., Zielinski, G.A., Vaars, A., Kukla, G., 1997. Asian provenance of glacial dust (stage 2) in the Greenland Ice Sheet Project 2 Ice Core, Summit, Greenland. J. Geophys. Res.-Oceans. 102, 26765-26781.

Bory, A.J.M., Biscaye, P.E., Svensson, A., Grousset, F.E., 2002. Seasonal variability in the origin of recent atmospheric mineral dust at NorthGRIP, Greenland. Earth Planet. Sc. Lett. 196, 123-134.

Bory, A.J.M., Biscaye, P.E., Grousset, F.E., 2003. Two distinct seasonal Asian source regions for mineral dust deposited in Greenland (NorthGRIP). Geophys. Res. Lett. 30, 1167, doi:10.1029/2002GL016446.

Brewer, P.G., Nozaki, Y., Spencer, D.W., Fleer, A.P., 1980. Sediment trap experiments in the deep North Atlantic: Isotopic and elemental fluxes. J. Mar. Res. 38, 703-728.

Cao, L.Q., Arculus, R.J., McKelvey, B.C., 1995a. Geochemistry and petrology of volcanic ashes recovered from Sites 881 through 884: A temporal record of Kamchatka and Kurile volcanism, in: Rea, D.K., Basov, I.A., Scholl, D.W., Allan, J.F. (Eds.), Proceedings of the Ocean Drilling Program, Scientific Results, Volume 145. Ocean Drilling Program, College Station, TX, pp. 345-381.

Cao, L.Q., Arculus, R.J., McKelvey, B.C., 1995b. Geochemistry of volcanic ashes recovered from Hole 887A, in: Rea, D.K., Basov, I.A., Scholl, D.W., Allan, J.F. (Eds.), Proceedings of the Ocean Drilling Program, Scientific Results, Volume 145. Ocean Drilling Program, College Station, TX, pp. 661-669.

Chen, Z.H., Gao, A.G., Liu, Y.G., Sun, H.Q., Shi, X.F., Yang, Z.S., 2003. REE geochemistry of surface sediments in the Chukchi Sea. Sci. China Ser. D 46, 603-611.

Condie, K.C., 1991. Another look at rare earth elements in shales. Geochim. Cosmochim. Ac. 55, 2527-2531.

Creamean, J.M., Suski, K.J., Rosenfeld, D., Cazorla, A., DeMott, P.J., Sullivan, R.C., White, A.B., Ralph, F.M., Minnis, P., Comstock, J.M., Tomlinson, J.M., Prather, K.A., 2013. Dust and Biological Aerosols from the Sahara and Asian Influence Precipitation in the Western U.S.. Science 339, 1572-1578.

Duce, R.A., Unni, C.K., Ray, B.J., Prospero, J.M., Merrill, J.T., 1980. Long-Range Atmospheric Transport of Soil Dust from Asia to the Tropical North Pacific: Temporal Variability. Science 209, 1522-1524.

Eguchi, K., Uno, I., Yumimoto, K., Takemura, T., Shimizu, A., Sugimoto, N., Liu, Z., 2009. Trans-pacific dust transport: integrated analysis of NASA/CALIPSO and a global aerosol transport model. Atmos. Chem. Phys. 9, 3137-3145.

Farley, K.A., 1995. Cenozoic variations in the flux of interplanetary dust recorded by ^{3}He in a deep-sea sediment. Nature 376, 153-156.

Farley, K.A., 2001. Extraterrestrial Helium in Seafloor Sediments: Identification, Characteristics, and Accretion Rate Over Geologic Time, in: Peucker-Ehrenbrink,

B., Schmitz, B. (Ed.), Accretion of Extraterrestrial Matter Throughout Earth's History. Kluwer Academic/Plenum Publishers, New York, NY, pp. 179-204.

Farley, K.A., Love, S.G., Patterson, D.B., 1997. Atmospheric entry heating and helium retentivity of interplanetary dust particles. Geochim. Cosmochim. Ac. 61, 2309-2316.

Ferrat, M., Weiss, D.J., Strekopytov, S., Dong, S.F., Chen, H.Y., Najorka, J., Sun, Y.B., Gupta, S., Tada, R., Sinha, R., 2011. Improved provenance tracing of Asian dust sources using rare earth elements and selected trace elements for palaeomonsoon studies on the eastern Tibetan Plateau. Geochim. Cosmochim. Ac. 75, 6374-6399.

Fleisher, M.Q., Anderson, R.F., 2003. Assessing the collection efficiency of Ross Sea sediment traps using ^{230}Th and ^{231}Pa. Deep-Sea Res. II 50, 693-712.

Francois, R., Frank, M., van der Loeff, M.M.R., Bacon, M.P., 2004. ^{230}Th normalization: An essential tool for interpreting sedimentary fluxes during the late Quaternary. Paleoceanography 19, PA1018, doi:10.1029/2003PA000939.

Fullam, T.J., Supko, P.R., Boyce, R.E., Stewart, R.W., 1973. Some aspects of Late Cenozoic sedimentation in the Bering Sea and North Pacific Ocean, in: Creager, J.S., Scholl, D.W., et al. (Eds.), Initial Reports of the Deep Sea Drilling Project, Volume 19. U.S. Government Printing Office, Washington, D.C., pp. 887-896.

Gale, A., Dalton, C.A., Langmuir, C.H., Su, Y.J., Schilling, J.G., 2013. The mean composition of ocean ridge basalts. Geochem. Geophys. Geosyst. 14, 489-518, doi:10.1002/GGGE20038.

Gallet, S., Jahn, B.M., Torii, M., 1996. Geochemical characterization of the Luochuan loess-paleosol sequence, China, and paleoclimatic implications. Chem. Geol. 133, 67-88.

Gallet, S., Jahn, B.M., Lanoë, B.V., Dia, A., Rossello, E., 1998. Loess geochemistry and its implications for particle origin and composition of the upper continental crust. Earth Planet. Sc. Lett. 156, 157-172.

Gutjahr, M., Frank, M., Stirling, C.H., Klemm, V., van de Flierdt, T., Halliday, A.N., 2007. Reliable extraction of a deepwater trace metal isotope signal from Fe-Mn oxyhydroxide coatings of marine sediments. Chem. Geol. 242, 351-370.

Hayes, C.T., Anderson, R.F., Fleisher, M.Q., Serno, S., Winckler, G., Gersonde, R., 2013. Quantifying lithogenic inputs to the North Pacific Ocean using the long-lived thorium isotopes. Earth Planet. Sc. Lett. 383, 16-25.

Henderson, G.M., Heinze, C., Anderson, R.F., Winguth, A.M.E., 1999. Global distribution of the ^{230}Th flux to ocean sediments constrained by GCM modelling. Deep-Sea Res. I 46, 1861-1893.

Herron, M.M., Matteson, A., 1993. Elemental Composition and Nuclear Parameters of Some Common Sedimentary Minerals. Nucl. Geophys. 7, 383-406.

Honda, M., Yabuki, S., Shimizu, H., 2004. Geochemical and isotopic studies of aeolian sediments in China. Sedimentology 51, 211-230.

Hsieh, Y.T., Henderson, G.M., Thomas, A.L., 2011. Combining seawater ^{232}Th and ^{230}Th concentrations to determine dust fluxes to the surface ocean. Earth Planet. Sc. Lett. 312, 280-290.

Hsu, S.C., Huh, C.A., Lin, C.Y., Chen, W.N., Mahowald, N.M., Liu, S.C., Chou, C.C.K., Liang, M.C., Tsai, C.J., Lin, F.J., Chen, J.P., Huang, Y.T., 2012. Dust transport from non-East Asian sources to the North Pacific. Geophys. Res. Lett. 39, L12804, doi:10.1029/2012GL051962.

Husar, R.B., Tratt, D.M., Schichtel, B.A., Falke, S.R., Li, F., Jaffe, D., Gasso, S., Gill, T., Laulainen, N.S., Lu, F., Reheis, M.C., Chun, Y., Westphal, D., Holben, B.N., Gueymard, C., McKendry, I., Kuring, N., Feldman, G.C., McClain, C., Frouin, R.J., Merrill, J., DuBois, D., Vignola, F., Murayama, T., Nickovic, S., Wilson, W.E., Sassen, K., Sugimoto, N., Malm, W.C., 2001. Asian dust events of April 1998. J. Geophys. Res.-Atmos. 106, 18317-18330.

Jones, C.E., Halliday, A.N., Rea, D.K., Owen, R.M., 1994. Neodymium isotopic variations in North Pacific modern silicate sediment and the insignificance of detrital REE contributions to seawater. Earth Planet. Sc. Lett. 127, 55-66.

Kohfeld, K.E., Chase, Z., 2011. Controls on deglacial changes in biogenic fluxes in the North Pacific Ocean. Quat. Sci. Rev. 30, 3350-3363.

Kurz, M.D., Curtice, J., Lott, D.E., Solow, A., 2004. Rapid helium isotopic variability in Mauna Kea shield lavas from the Hawaiian Scientific Drilling Project. Geochem. Geophy. Geosy. 5, Q04G14, doi:10.1029/2002GC000439.

Laurent, B., Marticorena, B., Bergametti, G., Chazette, P., Maignan, F., Schmechtig, C., 2005. Simulation of the mineral dust emission frequencies from desert areas of China and Mongolia using an aerodynamic roughness length map derived from the POLDER/ADEOS 1 surface products. J. Geophys. Res.-Atmos. 110, D18S04, doi:10.1029/2004JD005013.

Machalett, B., 2010. Past Atmospheric Circulation Patterns and Aeolian Dust Dynamics Recorded in Eurasian Loess: Utilizing high-resolution particle size

analysis and amino acid geochronology. Ph.D. Thesis, Humboldt-Universität zu Berlin, Germany.

Machalett, B., Oches, E.A., Frechen, M., Zller, L., Hambach, U., Mavkyanova, N.G., Markovic, S.B., Endlicher, W., 2008. Aeolian dust dynamics in central Asia during the Pleistocene: Driven by the long-term migration, seasonality, and permanency of the Asiatic polar front. Geochem. Geophys. Geosyst. 9, Q08Q09, doi:10.1029/2007GC001938.

Maeda, N., Noriki, S., Narita, H., 2007. Grain Size, La/Yb and Th/Sc of Settling Particles in the Western North Pacific: Evidence for Lateral Transport of Small Asian Loess. J. Oceanogr. 63, 803-812.

Mamyrin, B.A., Tolstikhin, I.N., 1984. Helium Isotopes in Nature. Elsevier, Amsterdam, Netherlands.

Marcantonio, F., Kumar, N., Stute, M., Andersen, R.F., Seidl, M.A., Schlosser, P., Mix, A., 1995. A comparative study of accumulation rates derived by He and Th isotope analysis of marine sediments. Earth Planet. Sc. Lett. 133, 549-555.

Marcantonio, F., Higgins, S., Anderson, R.F., Stute, M., Schlosser, P., Rasbury, E.T., 1998. Terrigenous helium in deep-sea sediments. Geochim. Cosmochim. Ac. 62, 1535-1543.

Marcantonio, F., Anderson, R.F., Higgins, S., Fleisher, M.Q., Stute, M., Schlosser, P., 2001. Abrupt intensification of the SW Indian Ocean monsoon during the last deglaciation: constraints from Th, Pa, and He isotopes. Earth Planet. Sc. Lett. 184, 505-514.

Marcantonio, F., Thomas, D.J., Woodard, S., McGee, D., Winckler, G., 2009. Extraterrestrial ^{3}He in Paleocene sediments from Shatsky Rise: Constraints on sedimentation rate variability. Earth Planet. Sc. Lett. 287, 24-30.

McGee, D., 2009. Reconstructing and interpreting the dust record and probing the plumbing of Mono Lake. Ph.D. Thesis, Columbia University, New York, NY.

McGee, D., Marcantonio, F., Lynch-Stieglitz, J., 2007. Deglacial changes in dust flux in the eastern equatorial Pacific. Earth Planet. Sc. Lett. 257, 215-230.

McGee, D., deMenocal, P.B., Winckler, G., Stuut, J.B., Bradtmiller, L.I., 2013. The magnitude, timing and abruptness of changes in North African dust deposition over the last 20,000 years. Earth Planet. Sc. Lett. 371, 163-176.

McKendry, I.G., Hacker, J.P., Stull, R., Sakiyama, S., Mignacca, D., Reid, K., 2001. Long-range transport of Asian dust to the Lower Fraser Valley, British Columbia, Canada. J. Geophys. Res.-Atmos. 106, 18361-18370.

McLennan, S.M., 1989. Rare earth elements in sedimentary rocks: Influence of provenance and sedimentary processes. Rev. Mineral. 21, 169-200.

Moreno, T., Querol, X., Castillo, S., Alastuey, A., Cuevas, E., Herrmann, L., Mounkaila, M., Elvira, J., Gibbons, W., 2006. Geochemical variations in aeolian mineral particles from the Sahara-Sahel Dust Corridor. Chemosphere 65, 261-270.

Mortlock, R.A., Froelich, P.N., 1989. A simple method for the rapid determination of biogenic opal in pelagic marine sediments. Deep-Sea Res. 36, 1415-1426.

Mukhopadhyay, S., Kreycik, P., 2008. Dust generation and drought patterns in Africa from helium-4 in a modern Cape Verde coral. Geophys. Res. Lett. 35, L20820, doi:10.1029/2008GL035722.

Mukhopadhyay, S., Farley, K.A., Montanari, A., 2001. A 35 Myr record of helium in pelagic limestones from Italy: Implications for interplanetary dust accretion from the early Maastrichtian to the middle Eocene. Geochim. Cosmochim. Ac. 65, 653-669.

Nagashima, K., Tada, R., Matsui, H., Irino, T., Tani, A., Toyoda, S., 2007. Orbital- and millennial-scale variations in Asian dust transport path to the Japan Sea. Palaeogeogr. Palaeoclimatol. Palaeoecol. 247, 144-161.

Nagashima, K., Tada, R., Tani, A., Sun, Y., Isozaki, Y., Toyoda, S., Hasegawa, H., 2011. Millennial-scale oscillations of the westerly jet path during the last glacial period. J. Asian Earth Sci. 40, 1214-1220.

Nakai, S., Halliday, A.N., Rea, D.K., 1993. Provenance of dust in the Pacific Ocean. Earth Planet. Sc. Lett. 119, 143-157.

Nakano, T., Yokoo, Y., Nishikawa, M., Koyanagi, H., 2004. Regional Sr-Nd isotopic ratios of soil minerals in northern China as Asian dust fingerprints. Atmos. Environ. 38, 3061-3067.

Nier, A.O., Schlutter, D.J., 1990. Helium and neon isotopes in stratospheric particles. Meteoritics 25, 263-267.

Nier, A.O., Schlutter, D.J., 1992. Extraction of helium from individual interplanetary dust particles by step-heating. Meteoritics 27, 166-173.

Olivarez, A.M., Owen, R.M., Rea, D.K., 1991. Geochemistry of eolian dust in Pacific pelagic sediments: Implications for paleoclimatic interpretations. Geochim. Cosmochim. Ac. 55, 2147-2158.

Opdyke, N.D., Foster, J.H., 1970. Paleomagnetism of cores from the North Pacific, in: Hays, J.D. (Ed.), Geological Investigations of the North Pacific. Geological Society of America, Boulder, CO, pp. 83-119.

Otosaka, S., Honda, M.C., Noriki, S., 2004. La/Yb and Th/Sc in settling particles: Vertical and horizontal transport of lithogenic material in the western North Pacific. Geochem. J. 38, 515-525.

Palmer, M.R., 1985. Rare earth elements in foraminifera tests. Earth Planet. Sc. Lett. 73, 285-298.

Patterson, D.B., Farley, K.A., Norman, M.D., 1999. ^{4}He as a tracer of continental dust: A 1.9 million year record of aeolian flux to the west equatorial Pacific Ocean. Geochim. Cosmochim. Ac. 63, 615-625

Prospero, J.M., Ginoux, P., Torres, O., Nicholson, S.E., Gill, T.E., 2002. Environmental characterization of global sources of atmospheric soil dust identified with the Nimbus 7 Total Ozone Mapping Spectrometer (TOMS) absorbing aerosol product. Rev. Geophys. 40, 1002, doi:10.1029/2000RG000095.

Pye, K., Zhou, L.P., 1989. Late Pleistocene and Holocene Aeolian Dust Deposition in North China and the Northwest Pacific Ocean. Palaeogeogr. Palaeocl. Palaeoecol. 73, 11-23.

Rea, D.K., Hovan, S.A., 1995. Grain size distribution and depositional processes of the mineral component of abyssal sediments: Lessons from the North Pacific. Paleoceanography 10, 251-258.

Roberts, N.L., Piotrowski, A.M., Elderfield, H., Eglinton, T.I., Lomas, M.W., 2012. Rare earth element association with foraminifera. Geochim. Cosmochim. Ac. 94, 57-71.

Ryan, W.B.F., Carbotte, S.M., Coplan, J.O., O'Hara, S., Melkonian, A., Arko, R., Weissel, R.A., Ferrini, V., Goodwillie, A., Nitsche, F., Bonczkowski, J., Zemsky, R., 2009. Global Multi-Resolution Topography synthesis. Geochem. Geophys. Geosyst. 10, Q03014, doi:10.1029/2008GC002332.

Scheidegger, K.F., Corliss, J.B., Jezek, P.A., Ninkovich, D., 1980. Compositions of deep-sea ash layers derived from North Pacific volcanic arcs: Variations in time and space. J. Volcanol. Geoth. Res. 7, 107-137.

Shigemitsu, M., Narita, H., Watanabe, Y.W., Harada, N., Tsunogai, S., 2007. Ba, Si, U, Al, Sc, La, Th, C and $^{13}C/^{12}C$ in a sediment core in the western subarctic Pacific as proxies of past biological production. Mar. Chem. 106, 442-455.

Steiger, R.H., Jäger, E., 1977. Subcommission on Geochronology: Convention on the Use of Decay Constants in Geochronology and Cosmochronology. Earth Planet. Sc. Lett. 36, 359-362.

Sun, D.H., Bloemendal, J., Rea, D.K., An, Z.S., Vandenberghe, J., Lu, H.Y., Su, R.X., Liu, T.S., 2004. Bimodal grain-size distribution of Chinese loess, and its palaeoclimatic implications. Catena 55, 325-340.

Sun, J.M., Zhang, M.Y., Liu, T.S., 2001. Spatial and temporal characteristics of dust storms in China and its surrounding regions, 1960-1999: Relations to source area and climate. J. Geophys. Res.-Atmos. 106, 10325-10333.

Sun, Y.B., Tada, R., Chen, J., Liu, Q.S., Toyoda, S., Tani, A., Ji, J.F., Isozaki, Y., 2008. Tracing the provenance of fine-grained dust deposited on the central Chinese Loess Plateau. Geophys. Res. Lett. 35, L01804, doi:10.1029/2007GL031672.

Svensson, A., Biscaye, P.E., Grousset, F.E., 2000. Characterization of late glacial continental dust in the Greenland Ice Core Project ice core. J. Geophys. Res.-Atmos. 105, 4637-4656.

Taguchi, K., Narita, H., 1995. ^{230}Th and ^{231}Pa distributions in surface sediments off Enshunada, Japan, in: Sakai, H., Nozaki, Y. (Eds.), Biogeochemical Processes and Ocean Flux in the western Pacific. Terra Scientific Publishing, Tokyo, Japan, pp. 375-382.

Tanaka, T.Y., Chiba, M., 2006. A numerical study of the contributions of dust source regions to the global dust budget. Global Planet. Change. 52, 88-104.

Taylor, J.R., 1997. An Introduction to Error Analysis, 2nd ed.. University Science Books, Sausalito, CA.

Taylor, S.R., McLennan, S.M., 1985. The Continental Crust: its Composition and Evolution. Blackwell Scientific Publications, Palo Alto, CA.

Torfstein, A., 2012. Size fractionation, reproducibility and provenance of helium isotopes in north-equatorial pacific pelagic clays. Earth Planet. Sc. Lett. 339-340, 151-163.

Uno, I., Eguchi, K., Yumimoto, K., Liu, Z., Hara, Y., Sugimoto, N., Shimizu, A., Takemura, T., 2011. Large Asian dust layers continuously reached North America in April 2010. Atmos. Chem. Phys. 11, 7333-7341.

VanLaningham, S., Pisias, N.G., Duncan, R.A., Clift, P.D., 2009. Glacial-interglacial sediment transport to the Meiji Drift, northwest Pacific Ocean: Evidence for timing of Beringian outwashing. Earth Planet. Sc. Lett. 277, 64-72.

Wang, X.M., Dong, Z.B., Zhang, J.W., Liu, L.C., 2004. Modern dust storms in China: an overview. J. Arid Environ. 58, 559-574.

Weber, E.T., Owen, R.M., Dickens, G.R., Halliday, A.N., Jones, C.E., Rea, D.K., 1996. Quantitative resolution of eolian continental crustal material and volcanic detritus in North Pacific surface sediment. Paleoceanography 11, 115-127.

Winckler, G., Fischer, H., 2006. 30,000 Years of Cosmic Dust in Antarctic Ice. Science 313, 491.

Winckler, G., Anderson, R.F., Schlosser, P., 2005. Equatorial Pacific productivity and dust flux during the mid-Pleistocene climate transition. Paleoceanography 20, PA4025, doi:10.1029/2005PA001177.

Winckler, G., Anderson, R.F., Fleisher, M.Q., McGee, D., Mahowald, N., 2008. Covariant Glacial-Interglacial Dust Fluxes in the Equatorial Pacific and Antarctica. Science 320, 93-96.

Woodard, S.C., Thomas, D.J., Marcantonio, F., 2012. Thorium-derived dust fluxes to the tropical Pacific Ocean, 58 Ma. Geochim. Cosmochim. Ac. 87, 194-209.

Yumimoto, K., Eguchi, K., Uno, I., Takemura, T., Liu, Z., Shimizu, A., Sugimoto, N., 2009. An elevated large-scale dust veil from the Taklimakan Desert: Intercontinental transport and three-dimensional structure as captured by CALIPSO and regional and global models. Atmos. Chem. Phys. 9, 8545-8558.

Zdanowicz, C., Hall, G., Vaive, J., Amelin, Y., Percival, J., Girard, I., Biscaye, P., Bory, A., 2006. Asian dustfall in the St. Elias Mountains, Yukon, Canada. Geochim. Cosmochim. Ac. 70, 3493-3507.

Zhang, X.Y., Arimoto, R., Zhu, G.H., Chen, T., Zhang, G.Y., 1998. Concentration, size-distribution and deposition of mineral aerosol over Chinese desert regions. Tellus 50B, 317-330.

Zhao, T.L., Gong, S.L., Zhang, X.Y., Blanchet, J.P., McKendry, I.G., Zhou, Z.J., 2006. A Simulated Climatology of Asian Dust Aerosol and Its Trans-Pacific Transport. Part I: Mean Climate and Validation. J. Climate 19, 88-103.

Zobeck, T.M., Gill, T.E., Popham, T.W., 1999. A two-parameter Weibull function to describe airborne dust particle size distributions. Earth Surf. Proc. Land. 24, 943-955.

Supplementary Figures

Figure S1. Grain size distributions of the three best-fit Weibull endmembers following the approach in McGee et al. (2013; EM1 in red, EM2 in black, EM3 in green), and of the mean residual of our fits to the samples (in brown).

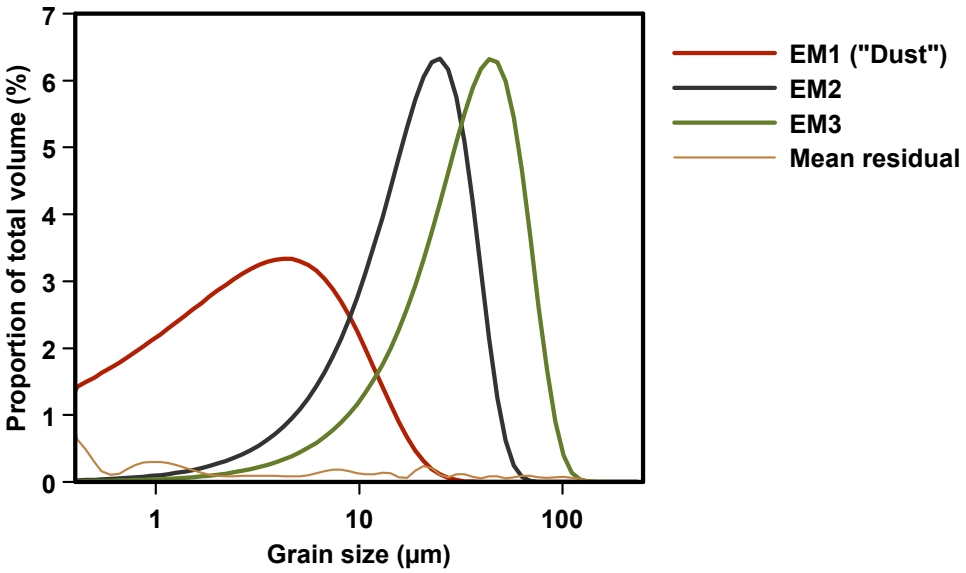

Figure S2. Location map of the East Asian dust source samples from the Taklimakan desert in black (TK-074, -083, -103 and -116), Inner Mongolia in red (BJ-024 from the Badain Jaran and TG-108 from the Tengger desert) and the Mongolian Gobi in blue (MG-06, -17 and -23; McGee, 2009; Ferrat et al., 2011). The map was created using GeoMapApp 3.0.1 (http://www.geomapapp.org) with the Global Multi-Resolution Topography synthesis (Ryan et al., 2009).

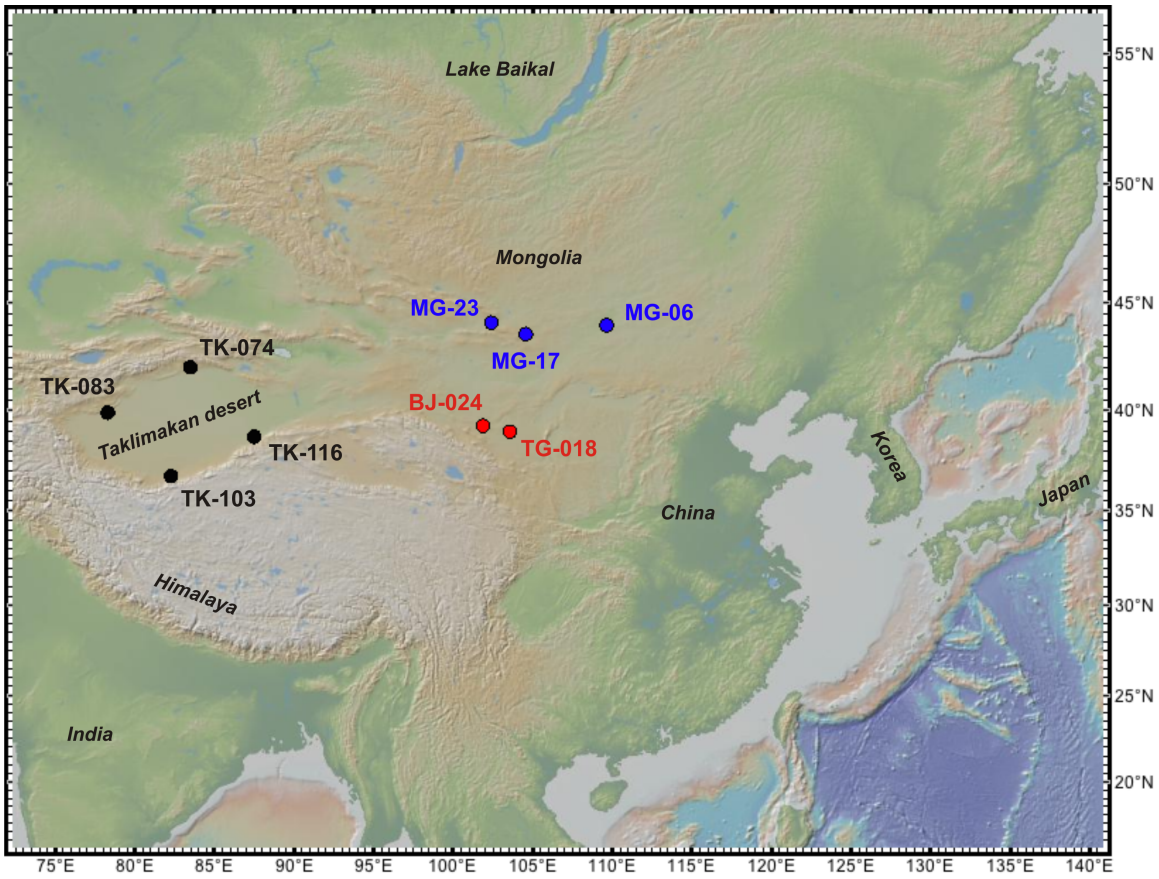

Figure S3. REE patterns for the mean East Asian dust endmember (top left), volcanic region 1 INOPEX samples from stations 1-3 and 31-45 (top right), volcanic region 2 samples from stations 4-9 (bottom left), and volcanic region 3 station samples 23-25 and 27-29 (bottom right). The values for each element were determined by normalizing the measured concentrations by the individual upper continental crust (UCC) values (Taylor and McLennan, 1985) and further normalizing the individual UCC-normalized elemental concentrations by the mean of all UCC-normalized REE values to better visualize differences in the patterns. The means for each element for the East Asian dust endmember are calculated from the 0-4, 4-8 and 4-16 μm size fractions of the dust source samples TK-074, TK-083, TK-103, BJ-024 and TG-018 (Ferrat et al., 2011; this study); presented uncertainties indicate the elemental standard deviations. The grey filled areas represent the ranges of the volcanic endmembers for each individual volcanic region based on the mean standard deviations calculated from compilations of volcanic ash layers from ODP sites 881, 882 and 887 (Cao et al., 1995a, b; Supplementary Information, Section 4.2).

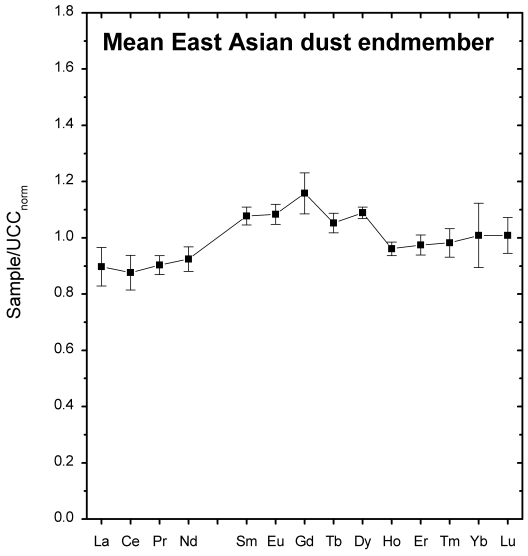
Mean East Asian dust endmember
Sample/UCC$_{norm}$
1.8
1.6
1.4
1.2
1.0
0.8
0.6
0.4
0.2
0.0
La Ce Pr Nd Sm Eu Gd Tb Dy Ho Er Tm Yb Lu

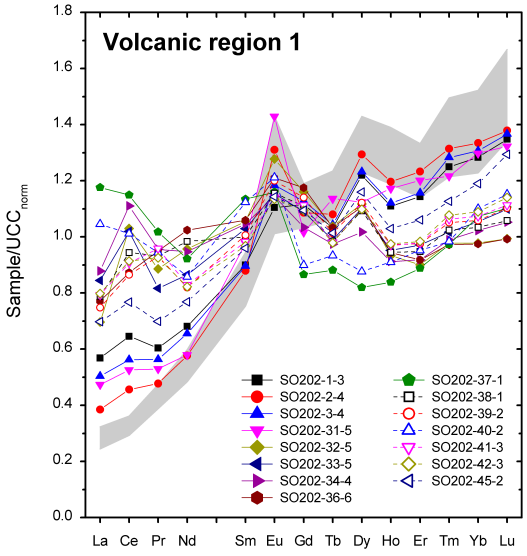
Volcanic region 1
Sample/UCC$_{norm}$
1.8
1.6
1.4
1.2
1.0
0.8
0.6
0.4
0.2
0.0
La Ce Pr Nd Sm Eu Gd Tb Dy Ho Er Tm Yb Lu
SO202-1-3
SO202-2-4
SO202-3-4
SO202-31-5
SO202-32-5
SO202-33-5
SO202-34-4
SO202-36-6
SO202-37-1
SO202-38-1
SO202-39-2
SO202-40-2
SO202-41-3
SO202-42-3
SO202-45-2

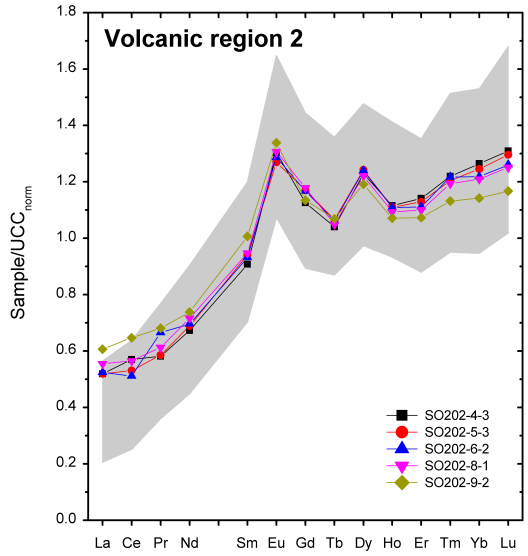
Volcanic region 2
Sample/UCC$_{norm}$
1.8
1.6
1.4
1.2
1.0
0.8
0.6
0.4
0.2
0.0
La Ce Pr Nd Sm Eu Gd Tb Dy Ho Er Tm Yb Lu
SO202-4-3
SO202-5-3
SO202-6-2
SO202-8-1
SO202-9-2

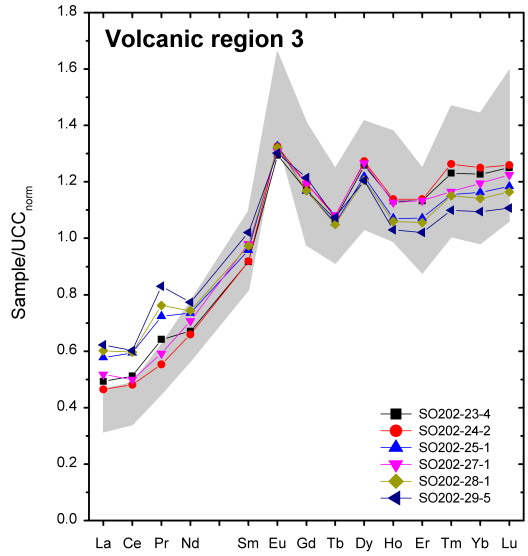
Volcanic region 3
Sample/UCC$_{norm}$
1.8
1.6
1.4
1.2
1.0
0.8
0.6
0.4
0.2
0.0
La Ce Pr Nd Sm Eu Gd Tb Dy Ho Er Tm Yb Lu
SO202-23-4
SO202-24-2
SO202-25-1
SO202-27-1
SO202-28-1
SO202-29-5

Supplementary Tables

Table S1. Linear sedimentation rates (LSR), LSR references (Ref.), contribution factors of Holocene eolian dust to the top cm in the marine sediments based on a simple bioturbation model (Section 3.3 in the main text), and measured (^{230}Th-normalized dust flux without correction for bioturbation) and modeled dust flux values (^{230}Th-normalized dust flux after correction for bioturbation) from the $^{4}He_{terr}$, ^{232}Th, REE and Weibull grain size modeling approaches for the deep station samples from the Southern Transect. Reference (1) = Opdyke and Foster (1970), Reference (2) = Lucia Korff, University of Bremen, personal communication.

Station	Dust approach	Dust flux [g/m^2/yr]	32	33	34	36	38	39	41	42	45
LSR [cm/kyr]			1.00	1.00	0.50	0.50	1.00	1.66	2.00	1.74	5.00
Ref.			(1)	(1)	(1)	(1)	(2)	(2)	(2)	(2)	(1)
Holocene dust fraction			0.838	0.838	0.748	0.748	0.838	0.922	0.966	0.933	1.000
	$^4He_{terr}$	*Measured*	2.475 ± 0.138	2.576 ± 0.253	2.254 ± 0.088	2.444 ± 0.102	2.650 ± 0.093	2.196 ± 0.119	1.750 ± 0.068	1.747 ± 0.096	2.370 ± 0.205
		Modeled	1.664 ± 0.499	1.732 ± 0.520	1.282 ± 0.385	1.390 ± 0.417	1.782 ± 0.535	1.780 ± 0.534	1.588 ± 0.476	1.453 ± 0.436	2.368 ± 0.710
	^{232}Th	*Measured*	2.057 ± 0.190	2.551 ± 0.221	2.254 ± 0.203	2.088 ± 0.188	2.579 ± 0.232	2.246 ± 0.212	2.298 ± 0.222	2.315 ± 0.233	3.049 ± 0.295
		Modeled	1.383 ± 0.415	1.715 ± 0.515	1.282 ± 0.385	1.188 ± 0.356	1.735 ± 0.520	1.821 ± 0.546	2.084 ± 0.625	1.925 ± 0.578	3.047 ± 0.914
	REE	*Measured*	2.529 ± 0.218	2.429 ± 0.190	2.254 ± 0.209	2.444 ± 0.212	2.893 ± 0.236	2.532 ± 0.206	2.838 ± 0.226	3.110 ± 0.253	3.365 ± 0.347
		Modeled	1.700 ± 0.510	1.634 ± 0.490	1.282 ± 0.385	1.390 ± 0.417	1.946 ± 0.584	2.053 ± 0.616	2.575 ± 0.772	2.586 ± 0.776	3.363 ± 1.009
	Grain size	*Measured*	2.149 ± 0.069	2.241 ± 0.073	2.164 ± 0.070	2.175 ± 0.068	2.715 ± 0.088	2.621 ± 0.086	3.028 ± 0.098	3.237 ± 0.103	4.201 ± 0.086
		Modeled	1.445 ± 0.434	1.507 ± 0.452	1.231 ± 0.369	1.237 ± 0.371	1.826 ± 0.548	2.125 ± 0.638	2.747 ± 0.824	2.692 ± 0.808	4.198 ± 1.259

Table S2. REE concentrations and recoveries of two certified reference rock samples, W-2 (U.S. Geological Survey) and JA-2 (Geological Survey of Japan). Recoveries are based on means of reported values from the GeoReM database for geological and environmental reference materials.

	W-2		JA-2	
Element	**Concentration [ppm]**	**Recovery [%]**	**Concentration [ppm]**	**Recovery [%]**
La	10.818	101.68	16.745	103.49
Ce	23.993	102.86	35.194	106.10
Pr	2.883	96.06	3.658	97.31
Nd	12.813	99.39	14.493	101.66
Sm	3.280	98.94	3.123	102.57
Eu	1.120	102.34	0.929	102.73
Tb	0.592	95.51	0.478	101.51
Gd	3.749	102.17	3.120	104.09
Dy	3.887	103.05	3.021	104.20
Ho	0.794	100.88	0.616	104.18
Er	2.254	102.24	1.767	104.47
Tm	0.323	98.66	0.259	100.25
Yb	2.145	104.73	1.758	106.09
Lu	0.308	98.56	0.259	100.53